Processing and Mechanical Properties of Fluorinated Single-Wall Carbon Nanotube−Polyethylene Composites

Meisha L. Shofner,[†,#] Valery N. Khabashesku,*[,‡] and Enrique V. Barrera*[,†]

Department of Mechanical Engineering and Materials Science, and Department of Chemistry and Center for Nanoscale Science and Technology, Rice University, Houston, Texas 77005-1892

Received July 7, 2005. Revised Manuscript Received November 22, 2005

To efficiently reinforce polymer matrix composites with carbon nanotubes, issues of dispersion and nanotube−matrix compatibility should be optimized. Sidewall chemical functionalization was shown to be effective in improving both the dispersion and interaction between the nanotube and the matrix. This work evaluates the affect of sidewall functional group on dispersing the fluorinated single-walled carbon nanotubes (F−SWNTs) in a thermoplastic matrix (polyethylene) and on the mechanical properties of the F−SWNT composites fabricated. These studies demonstrate that in comparison with polyethylene composites, filled with purified nanotubes, improved dispersion and interfacial and mechanical properties are achieved for F−SWNT-loaded matrixes due to chemical functionalization. In addition, the observed partial removal of functional groups from the F−SWNTs during melt processing with polyethylene by shear mixing suggests a possibility of in situ direct covalent bonding between the nanotubes and the matrix which ultimately results in mechanical reinforcement of the composite.

Introduction

Single-wall carbon nanotubes (SWNTs) have great potential for reinforcement of polymer matrix composites since they inherently possess high strength and high thermal and electrical conductivities.[1−3] However, roping and a chemically inert structure inhibit load transfer by the SWNTs, limiting the mechanical property improvements. The atomically smooth structure surface of SWNTs results in a low reactivity, and van der Waals attractive forces between individual nanotubes cause the nanotubes to assemble into a hexagonal arrangement forming long ropes of nanotubes. These ropes generally have diameters that are 1 or 2 orders of magnitude larger than an individual SWNT and lengths of several micrometers.[3] Ineffective interfacial bonding and sliding of individual nanotubes within the ropes inhibit load transfer from the matrix to the fiber, limiting the amount of mechanical reinforcement achievable in polymer matrix composites.[4] Therefore, the diameter of the rope is directly related to its load carrying capacity.[1] Individual nanotubes are expected to provide the most reinforcement. Functionalization of the nanotube surface is a method to introduce reactive moieties, to disrupt the rope structure, and to obtain smaller diameter ropes and possibly individual nanotubes. Functionalization will also serve to separate nanotubes by type (e.g., semiconducting vs metallic) so that future composite systems will use nanotubes of a specific type to foster enhanced properties.[5] Functional moieties are attached to open ends and sidewalls, primarily to improve the solubility of nanotubes.[6−14] Among these methods, fluorination[13] is one of the few methods that is easily scalable and does not require a solvent for the functionalization reaction to take place. Improved dispersion of fluorinated nanotubes in composites and increased mechanical properties have already been observed in the works of Zhu et al.[15] and Geng et al.,[16] in epoxy and poly(ethylene oxide) matrixes, respectively.

* Corresponding authors. E-mail: khval@rice.edu (V.N.K.); ebarrera@rice.edu (E.V.B.).

† Department of Mechanical Engineering and Materials Science.

Current address: School of Polymer, Textile and Fiber Engineering, Georgia Institute of Technology, Atlanta, GA 30332.

‡ Department of Chemistry and Center for Nanoscale Science and Technology.

(1) Yu, M. F.; Files, B. S.; Arepalli, S.; Ruoff, R. S. *Phys. Rev. Lett.* **2000**, *84*, 5552.
(2) Hone, J.; Liaguno, M. C.; Nemes, N. M.; Johnson, A. T.; Fischer, J. E.; Walters, D. A.; Casavant, M. J.; Schmidt, J.; Smalley, R. E. *Appl. Phys. Lett.* **2000**, *77*, 666.
(3) Thess, A.; Lee, R.; Nikolaev, P.; Dai, H.; Petit, P.; Robert, J.; Xu, C.; Lee, Y. H.; Kim, S. G.; Rinzler, A. G.; Colbert, D. T.; Scuseria, G. E.; Tomanek, D.; Fischer, J. E.; Smalley, R. E. *Science* **1996**, *273*, 483.
(4) Ajayan, P. M.; Schadler, L. S.; Giannaris, C.; Rubio, A. *Adv. Mater.* **2000**, *12*, 750.
(5) Dyke, C. A.; Stewart, M. P.; Tour, J. M. *J. Am. Chem. Soc.* **2005**, *127*, 4498.
(6) Boul, P. J.; Liu, J.; Mickelson, E. T.; Huffman, C. B.; Ericson, L. M.; Chiang, I. W.; Smith, K. A.; Colbert, D. T.; Hauge, R. H.; Margrave, J. L.; Smalley, R. E. *Chem. Phys. Lett.* **1999**, *310*, 367.
(7) Bahr, J. L.; Tour, J. M. *Chem. Mater.* **2001**, *13*, 3823.
(8) Chen, Y.; Haddon, R. C.; Fang, S.; Rao, A. M.; Eklund, P. C.; Lee, W. H.; Dickey, E. C.; Grulke, E. A.; Pendergrass, J. C.; Chavan, A.; Haley, B. E.; Smalley, R. E. *J. Mater. Res.* **1998**, *13*, 2423.
(9) Georgakilas, V.; Kordatos, K.; Prato, M.; Guldi, D. M.; Holzinger, M.; Hirsch, A. *J. Am. Chem.* Soc. **2002**, *124*, 760.
(10) Liu, J.; Rinzler, A. G.; Dai, H.; Hafner, J. H.; Bradley, R. K.; Boul, P. J.; Lu, A.; Iverson, T.; Shelimov, K.; Huffman, C. B.; Rodriguez-Macias, F.; Shon, Y.-S.; Lee, T. R.; Colbert, D. T.; Smalley, R. E. *Science* **1998**, *280*, 1253.
(11) Mickelson, E. T.; Huffman, C. B.; Rinzler, A. G.; Smalley, R. E.; Hauge, R. H.; Margrave, J. L. *Chem. Phys. Lett.* **1998**, *296*, 188.
(12) Peng, H.; Reverdy, P.; Khabashesku, V. N.; Margrave, J. L. *Chem. Commun.* **2003**, 362.
(13) Wong, S. S.; Woolley, A. T.; Joselevich, E.; Cheung, C. L.; Lieber, C. M. *J. Am. Chem. Soc.* **1998**, *120*, 8557.
(14) O'Connell, M. J.; Boul, P. J.; Ericson, L. M.; Huffman, C. B.; Wang, Y.; Haroz, E.; Kuper, C.; Tour, J. M.; Ausman, K.; Smalley, R. E. *Chem. Phys. Lett.* **2001**, *342*, 265.
(15) Zhu, J.; Kim, J. D.; Peng, H.; Margrave, J. L.; Khabashesku, V. N.; Barrera, E. V. *Nano Lett.* **2003**, *3*, 1107.

10.1021/cm051475y CCC: $33.50
Published on Web 01/21/2006

This paper describes the use of chemical functionalization of SWNTs, particularly fluorination, to address the problems of both dispersion and interaction between the nanotube and the matrix in a polyethylene matrix. The processing, nanotube/matrix interaction, dynamic mechanical properties, and thermal degradation of polyethylene matrix composites containing fluorinated SWNTs (F−SWNTs) are compared to those of composites containing purified SWNTs (P−SWNTs). The analysis shows that the fluorine functional groups enhance the interaction with polyethylene, improve the dispersion of nanotubes in the matrix, and increase the dynamic mechanical properties when compared to the composites containing P−SWNTs. The thermal decomposition pattern of the F−SWNTs is changed by the surrounding polymer matrix compared to a polymer-free condition. The removal of fluorine from the F−SWNTs does not lead to shortened nanotubes as in the absence of a matrix.[17] Instead, the liberated fluorine groups may attack the polyethylene chain to form HF and radical sites, creating an opportunity for grafting of the polymer to the nanotubes surface via direct covalent bonding. This can provide a new method for in situ design of fully integrated nanotube composites.[18]

This work also complements the two previous efforts[15,16] by providing insight into the thermal stability of the fluorine functional group on nanotubes and into the thermal decomposition of composites containing F−SWNTs. A method of implementing functionalization is proposed where in situ manipulation of functionalized nanotubes and their incorporation into a polymer matrix enables a host of composite properties.

Experimental Section

The polymer used as a matrix for composite fabrication in this work is a medium-density polyethylene powder purchased from Aldrich. The polymer has a density of 0.94 g/cm^3, a melting point range of 109−111 °C, and a molecular weight of approximately 6000. Polyethylene is chosen as the matrix because this study is part of a more comprehensive effort to develop lightweight radiation shielding using nanotube composites.[19] The SWNTs used in this research are obtained from Carbon Nanotechnologies, Inc. (Houston, Texas) in purified form[20] and produced by the HiPco method.[21] The SWNTs were supplied as a fluffy powder. TGA in flowing air indicates that these nanotubes have a residual metal catalyst content of 6 wt %. A portion of these purified nanotubes (P−SWNTs) were subsequently fluorinated to an approximately C_2F stoichiometry (F−SWNTs) according to published techniques that have established this stoichiometry as the maximum degree of fluorination achievable without permanently destroying the nanotube structure.[11,22]

The chemical composition and bonding structure of the nanotubes prior to composite processing was characterized with the XPS and Raman spectroscopy. XPS measurements were carried out using a Physical Electronics 5700 instrument and nonmonochromatic Al Kα incident radiation. Survey scans were done to identify the peaks of interest, and then high-resolution scans of these peaks were conducted on each sample. Raman spectroscopy measurements were performed using a Renishaw MicroRaman spectrometer with 780.6 nm laser and a resolution of 2 cm^{-1}. The microscope 50× objective with a 0.55 μm aperture was used.

To fabricate the composite materials from the two components, nanotubes F−SWNTs or P−SWNTs and polyethylene, a multistep processing procedure was used. The steps included dispersion of SWNTs into solvent to disrupt large agglomerates, incipient wetting, high shear mixing, and heated compression molding. The final product resulting from these processing and fabrication steps was a flat sheet of composite material that is approximately 100 mm square and 1 mm thick. Both the P−SWNTs and F−SWNTs were combined with alcohol solvents to create a suspension. Alcohol solvents were used for this study because their boiling points are lower than the melting point of the polymer, so the solvent can be evaporated without melting the polymer.

The P−SWNT suspensions have been prepared by sonication for several minutes in 2-propanol or tertiary butanol. The F−SWNT suspensions were prepared by magnetic stirring over several days. Since the F−SWNTs show a decreased solubility in tertiary butanol, 2-propanol was the only solvent used with the F−SWNTs. The SWNT suspensions were combined with the polyethylene to overcoat the polymer powder and create an initial dispersion between the polymer and the SWNTs.[18,23,24] Then the polyethylene powder/SWNT suspension mixture was heated in an oil bath at temperatures between 70 and 80 °C and dried in a vacuum oven at 80 °C to remove the solvent. The overcoated, dried powder has a uniform gray color, and the individual polymer powder particles do not agglomerate after the incipient wetting process. The overcoated powder was compounded by high shear mixing with a HAAKE Polylab System using a 30 g mixing bowl. The material was mixed at a speed of 150 rpm, temperature of 115 °C, and residence time of 10 min. After mixing, the material was formed into sheets using heated compression molding at 110 °C for 5 min with an applied force of 6−10 metric tons. The following compositions have been prepared: 1.5 wt % F−SWNT/polyethylene, 5 wt % F−SWNT/polyethylene, 1.5 wt % P−SWNT/polyethylene, 5 wt % P−SWNT/polyethylene, and neat polyethylene.

The interaction between the SWNTs and polyethylene after processing steps was evaluated by SEM imaging, Raman spectroscopy, TGA, Fourier transform infrared spectroscopy (FTIR), and dynamic mechanical analysis (DMA). The SEM studies were performed with a Phillips Electroscan ESEM XL30 instrument. To prevent sample surface charging all composite and neat polymer samples were coated with gold prior to analyses. The free-standing nanotube samples were imaged without gold coating. The TGA experiments were conducted using a TA Instruments SDT 2960 device, while the TGA−FTIR studies were performed on a TA Instruments Q500 TGA coupled to a Thermo-Nicolet Nexus 670 FTIR spectrometer. Both types of TGA experiments were done in flowing nitrogen at a heating rate of 10 °C/min. The residue from

(16) Geng, H.; Rosen, R.; Zheng, B.; Shimoda, H.; Fleming, L.; Liu, J.; Zhou, O. *Adv. Mater.* **2002**, *14*, 1388.
(17) Gu, Z.; Peng, H.; Hauge, R. H.; Smalley, R. E.; Margrave, J. L. *Nano Lett.* **2002**, *2*, 1009.
(18) Barrera, E. V. *JOM* **2000**, *52*, 38.
(19) Pulikkathara, M. X.; Shofner, M. L.; Wilkins, R. T.; Vera, J. G.; Barrera, E. V.; Rodriguez-Macias, F. J.; Vaidyanathan, R. K.; Green, C. E.; Condon, C. G. *Mater. Res. Soc. Symp. Proc.* **2003**, *740*, 365.
(20) Chiang, I. W.; Brinson, B. E.; Huang, A. Y.; Willis, P. A.; Bronikowski, M. J.; Margrave, J. L.; Smalley, R. E.; Hauge, R. H. *J. Phys. Chem. B* **2001**, *105*, 8297.
(21) Bronikowski, M.; Willis, P. A.; Colbert, D. T.; Smith, K. A.; Smalley, R. E. *J. Vac. Sci. Technol., A* **2001**, *19*, 1800.
(22) Chiang, I. W.; Saini, R. K.; Mickelson, E. T.; Billups, W. E.; Hauge, R. H.; Margrave, J. L. In *Proceedings of the Sixth Applied Diamond Conference/Second Frontier Carbon Joint Conference*; Tzeng, Y., Miyoshi, K., Yoshikawa, M., Murakawa, M., Koga, Y., Kobashi, K., Amaratunga, G. A. J., Eds.; NASA Glenn Research Center: Auburn, AL, 2001; p 687.
(23) Cooper, C. A.; Ravich, D.; Lips, D.; Mayer, J.; Wagner, H. D. *Compos. Sci. Technol.* **2002**, *62*, 1105.
(24) Haggenmueller, R.; Zhou, W.; Fischer, J. E.; Winey, K. I. *J. Nanosci. Nanotechnol.* **2003**, *3*, 105.

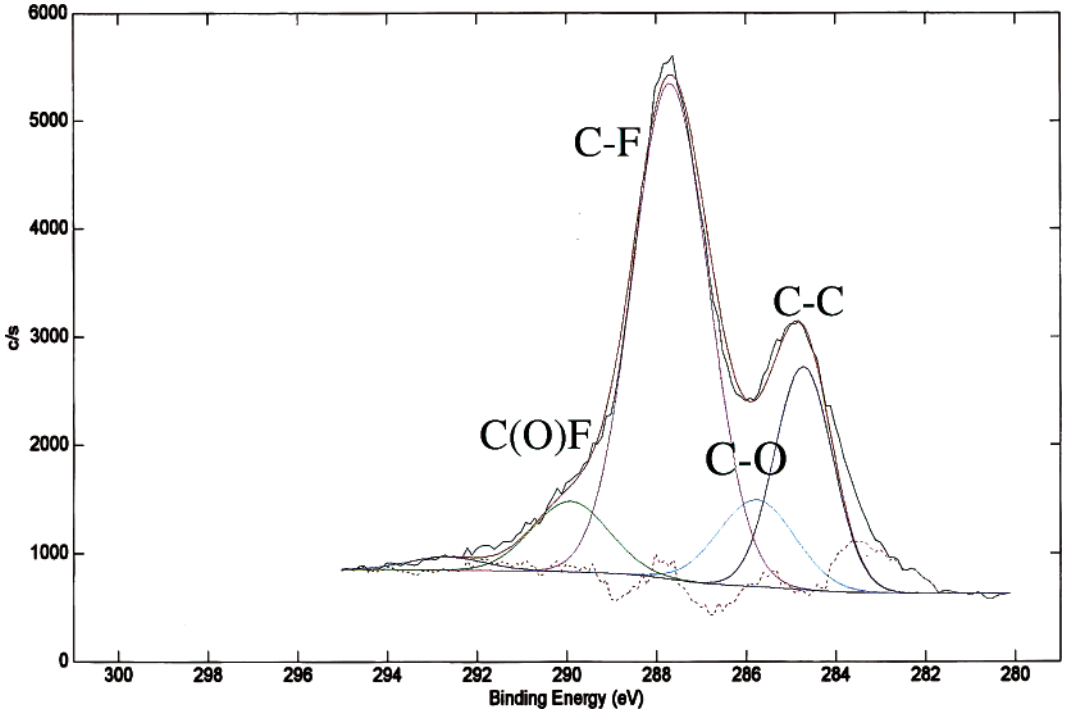

Figure 1. XPS C1s curve for the F−SWNT sample. The observed peaks are due to the change in carbon states from the sp^2 to sp^3 states after fluorination of P−SWNT to F−SWNT of approximately C_2F stoichiometry.

the TGA tests was normally collected for further study. Dynamic mechanical analysis (DMA) measurements were performed using a Perkin-Elmer Diamond DMA system. All tests were conducted in tension mode on film samples with an approximate thickness of 0.25 mm at a frequency of 1 Hz over a temperature range of 20 to −40 °C.

Results and Discussion

XPS analysis of the P−SWNTs and F−SWNTs done prior to incorporating the nanotubes into polymer matrix shows the elements present in the nanotubes before and after their functionalization through fluorination. The presence of carbon and oxygen in the P−SWNTs, and carbon, fluorine, and oxygen in the F−SWNTs has been established. The C1s scan of the P−SWNTs showed peaks of the sp^2 carbons at 284.8 eV, oxygen-grafted carbons in the form of hydroxyl and carboxyl groups at 286.1 and 288.3 eV, and a $\pi-\pi^*$ shake-up peak at 290.6 eV.[25,26] The oxygen-grafted carbon states are formed during the oxidizing acid treatment step in the purification procedure of the SWNTs.[27] The high-resolution C1s peak scan of the F−SWNTs (Figure 1) also shows carbons at 284.7 eV and oxygen-bonded carbons at 285.8 eV. Two peaks characteristic of fluorinated and oxofluorinated carbons are observed at 287.7 and 289.3 eV, respectively.[28] Analysis of the peaks produced elemental contents of carbon and fluorine in the F−SWNTs consistent with the stoichiometry of approximately C_2F.[29]

The nanotube sidewall chemical functionalization lead to changes in the dispersion characteristics between P−SWNTs and F−SWNTs. The addition of a fluorine functional group to the SWNTs significantly improves the dispersion of the nanotubes in the polyethylene matrix when compared to the composites containing P−SWNTs. The improvement in dispersion is evident from SEM imaging and from the mixing behavior of the composites. As shown in Figure 2, the F−SWNTs appear in the SEM images as smaller separated ropes, whereas the P−SWNTs are observed as agglomerated bundles divided by regions containing no nanotubes. The two solvents used in this work produce the same mixing and dispersion behavior for the P−SWNTs despite an increased solubility of P−SWNTs in tertiary butanol.

However, the P−SWNTs and F−SWNTs show their differences in behavior during the shear mixing processing with polyethylene into composites. The low molecular weight and narrow melting point range of the polyethylene results in a low melt viscosity of the composite which allows the effect of functionalization on dispersion to be studied without a significant contribution from shear forces. The viscosity, evidenced by mixing torque, is observed to increase with increasing nanotube loading in the polyethylene matrix, but the same loading of F−SWNTs causes a larger increase in the melt viscosity than in the case of P−SWNTs, as shown in Figure 3. The greater mixing torque of the F−SWNT materials is not intuitive because of differences in actual carbon nanotube content. The composition of the F−SWNTs

(25) Hiura, H.; Ebbesen, T. W.; Tanigaki, K. *Adv. Mater.* **1995**, *7*, 275.
(26) Viswanathan, H.; Rooke, M. A.; Sherwood, P. M. A. *Surf. Interface Anal.* **1997**, *25*, 409.
(27) Rinzler, A. G.; Liu, J.; Dai, H.; Nikolaev, P.; Huffman, C. B.; Rodríguez-Macías, F. J.; Boul, P. J.; Lu, A. H.; Heymann, D.; Colbert, D. T.; Lee, R. S.; Fischer, J. E.; Rao, A. M.; Eckland, P. C.; Smalley, R. E. *Appl. Phys. A* **1998**, *67*, 29.
(28) Mickelson, E. T. Novel Chemistry of Elemental Carbon: Graphite, Fullerenes and Nanotubes. Ph.D. Thesis, Rice University, Houston, Texas, 1999.
(29) Marcoux, P. R.; Schreiber, J.; Batail, P.; Lefrant, S.; Renouard, J.; Jacob, G.; Albertini, D.; Mevellec, J.-Y. *PhysChemChemPhys* **2002**, *4*, 2278.

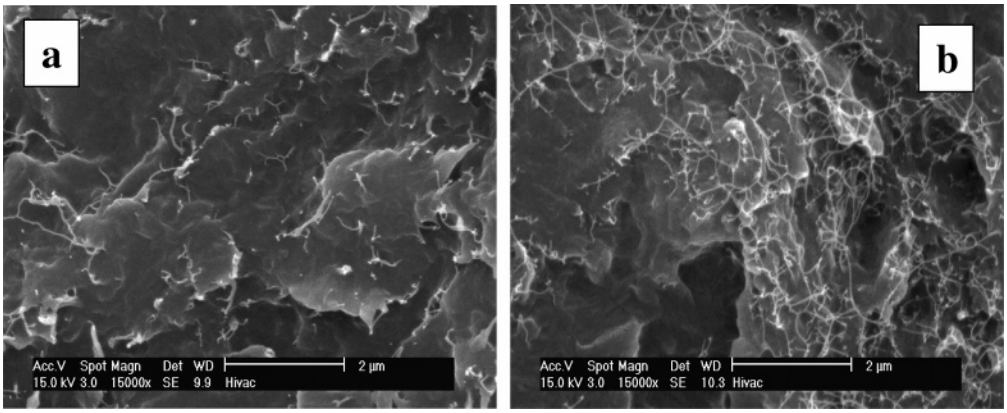

Figure 2. SEM images of the composite samples: 5 wt % F−SWNT/polyethylene (a) and 5 wt % P−SWNT/polyethylene (b). The F−SWNTs show an improved dispersion.

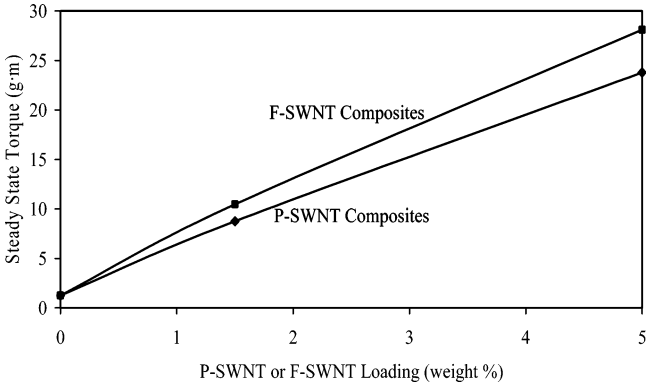

Figure 3. Mixing torque observed for neat polyethylene and SWNT composites. The mixing torque is greater in F−SWNT/polyethylene composites despite lower carbon nanotube content, indicating that the fluorination creates a larger number of smaller nanotube ropes.

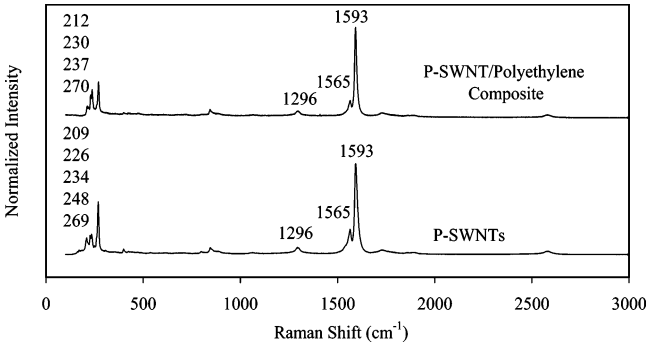

Figure 4. Raman spectra of P−SWNTs and P−SWNT/polyethylene composite. No compressive stresses are imposed upon nanotubes by the surrounding polymer matrix; therefore, no significant shifts are observed.

includes the weight of the fluorine functional groups, so the composite materials loaded with F−SWNTs have less carbon nanotube weight component than the composites prepared with the same loading of P−SWNT. The 1.5 wt % and 5 wt % F−SWNT composites contain approximately 0.8 wt % and 2.8 wt % SWNTs, respectively. Previous studies show that melt viscosity increases with nanotube loading,[30,31] so the higher SWNT content in the P−SWNT composites is expected to produce the larger torque. However, fluorination disrupts the larger bundles of nanotubes; therefore, a greater numbers of smaller ropes and possibly individual nanotubes act similarly to a larger loading of nanotubes. Also, the fluorine groups on the nanotube surface create a driving force for better dispersion by repulsing other surface fluorine groups.[29,32]

Differences between the P−SWNT and F−SWNT composites are also evident when the electronic structure of the nanotubes is probed by Raman spectroscopy at each processing step. The radial breathing modes in the range of 200−300 cm^{-1}, the disorder mode at approximately 1300 cm^{-1} indicative of sidewall defects in the form of sp^3 carbon bonding, and the tangential sp^2 carbon−carbon bond stretching mode near 1590 cm^{-1} are used to evaluate the interaction between the nanotubes and the polymer. The Raman spectra of P−SWNT−polyethylene composites show no remarkable changes when compared with those of the P−SWNTs (Figure 4). The nanotubes seem unaffected by the presence of the polymer matrix though an upshift of 3−4 cm^{-1} in three of the dominant radial breathing modes is observed. This shift is not considered significant because previous work has shown that both the radial breathing and tangential stretching modes experience a vibrational energy upshift only when nanotubes are loaded by hydrostatic compressive pressure.[33] Like the tangential stretching mode, the disorder mode in nanotubes remains unchanged by the presence of polyethylene.

In contrast, the F−SWNTs display a substantial interaction with the polyethylene matrix observed by Raman spectroscopy. The F−SWNTs and their composites demonstrate dramatic changes in comparison with the P−SWNTs through the processing as shown in Figure 5. The Raman features of the P−SWNTs become altered after the fluorination since the bonding states of the carbon atoms largely change from the sp^2 to sp^3 due to covalent bonding of fluorine to graphene surface of nanotubes.[29,32] The sp^2 carbon peak of the graphene π-system at 1592 cm^{-1} disappears, while a broad feature at 1580 cm^{-1} due to a disrupted aromatic π-conjugation and the increased intensity of the disorder mode are observed in the Raman spectrum of F−SWNTs. The vibrational energy

(30) Haggenmueller, R.; Gommans, H. H.; Rinzler, A. G.; Fischer, J. E.; Winey, K. I. *Chem. Phys. Lett.* **2000**, *330*, 219.
(31) Potschke, P.; Fornes, T. D.; Paul, D. R. *Polymer* **2002**, *43*, 3247.
(32) Mickelson, E. T.; Chiang, I. W.; Zimmerman, J. L.; Boul, P. J.; Lozano, J.; Liu, J.; Smalley, R. E.; Hauge, R. H.; Margrave, J. L. *J. Phys. Chem. B* **1999**, *103*, 4318.
(33) Venkateswaran, U. D.; Rao, A. M.; Richter, E.; Menon, M.; Rinzler, A. G.; Smalley, R. E.; Eklund, P. C. *Phys. Rev. B* **1999**, *59*, 10928.

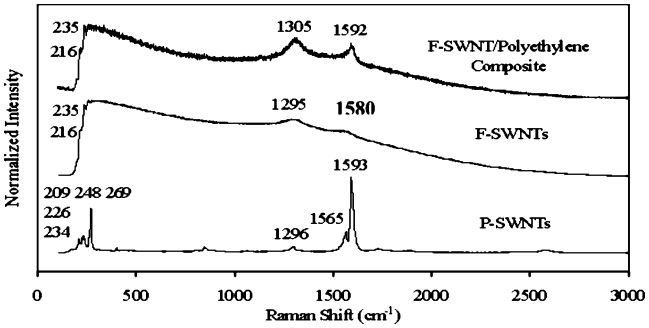

Figure 5. Raman spectra of P−SWNTs, F−SWNTs, and F−SWNT/polyethylene composite. The addition of fluorine to the nanotube sidewalls reduces the intensity of the sp^2 C=C stretching mode and increases the intensity of the sp^3 C−C stretching mode. After mixing and melt processing, some of the fluorine is removed from the nanotubes, as evidenced by the return of the sp^2 peak at 1592 cm^{-1}. The observed 10 cm^{-1} upshift in the sp^3 C−C stretching mode of the SWNT can likely be related to the nanotubes becoming covalently bonded to the polymer chains.

of the latter mode does not change appreciably because the difference between the electron-withdrawing−donating properties of oxygenated functional groups on the sidewalls of the oxidized SWNTs and that of fluorine functional groups is apparently not significant. The breathing modes in the F−SWNTs are obscured by the background and show only two defined peaks. After compounding with the polyethylene, these breathing modes do not change relative to those of the F−SWNTs. However, the observed changes in the disorder mode and tangential mode suggest that two events occurred: partial loss of fluorine (defluorination) and subsequent direct covalent bonding between the nanotube and the polymer.

Partial defluorination is supported by the return of the sp^2 peak at 1592 cm^{-1}, indicating a restoration of the π-electron graphene structure for the sections of sidewall. It seems unlikely that complete defluorination takes place under processing conditions studied since large background scattering typical for fluorinated nanotubes is still prominent in the Raman spectrum, and the intensity of the sp^2 peak is quite low compared to that of the P−SWNT/polyethylene composite shown in Figure 4. On the basis of the current knowledge, partial fluorine loss can be explained by two possible scenarios. First, certain diameter sizes or chiralities of nanotubes could lose different amounts of their fluorine functional groups. SWNT material produced by the HiPco process contains nanotubes of many different diameters indicated in the Raman spectrum by the radial breathing mode frequencies, so varying defluorination rate for the nanotubes with certain size and helicity is not improbable. Computational and experimental results have shown that the formation and stability of the C−F bond is related to the latter nanotube characteristics. Chiang et al.[22] have found that the fluorination reaction is also dependent on nanotube diameter. As the nanotube diameter decreases, the fluorination process occurs at lower temperatures and shorter times because the higher curvature of the smaller diameter nanotubes makes them more reactive. Computational results by Bettinger et al.[34] and Kudin et al.[35] find that the C−F bond

Scheme 1. Suggested Covalent Bonding of Polyethylene to F−SWNTs during Shear Mixing Processing

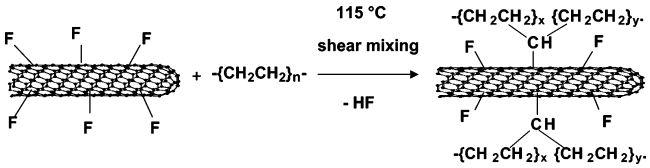

dissociation energy and nanotube diameter are inversely related. Jaffe[36] adds to this result by investigating the effect of chirality. His work suggests that zigzag nanotubes form stronger bonds with fluorine. Experimental research performed by Pulikkathara et al.[19] concerning composites containing F−SWNTs exposed to radiation shows a higher functional group stability for larger diameter nanotubes. Work is in progress to investigate the mechanism of radiation-induced transformations of functionalized SWNTs.[37] Combined, the studies done so far do not identify the mechanisms observed, but they do consider the possibility of preferred defluorination based on nanotube diameter or helicity.

The additional explanation for the partial loss of fluorine taking place during the shear mixing is defluorination of the outside surfaces of the nanotube ropes. Even though fluorination disrupts larger ropes, the nanotubes are still contained in a smaller diameter ropes as seen in Figure 2. Since the defluorination product is HF and the hydrogen is removed from the polyethylene matrix, fluorine groups brought in close contact with the polymer chain by applied shear force would be the most likely to be removed. Polymer chains do not penetrate the SWNT ropes, so internal surfaces are not in proximity to the polymer. Hence, the loss of fluorine from the outside rope surface is likely to contribute into partial defluorination mechanism. This does not contradict the explanation given before since nanotube surfaces of certain curvature and chirality exposed to the polymer could also lose fluorine while the functional groups on the corresponding surfaces inside the rope may not be affected.

The suggested formation of covalent bonds between the carbon atoms of the polyethylene and the nanotube resulting from intermolecular loss of HF is supported by the observed Raman shift in the disorder mode from 1295 to 1305 cm^{-1} (Figure 5). Carbon is lighter than fluorine, so the sp^3 Raman peak shifts to a higher frequency in comparison with the F−SWNTs. The opportunity for the covalent bonds to form can occur when in the course of applying heat and shear force simultaneously the fluorine groups are detached from the nanotube. Liberated fluorine atoms can attack the polyethylene and scavenge hydrogen to form HF gas. When hydrogens are removed from the chain, the open radical sites on the polymer can combine with the radical sites on the F−SWNTs creating new sp^3 carbon−carbon bonds which provide covalent bonding of the polyethylene chains to the nanotube sidewall (Scheme 1).

(34) Bettinger, H. F.; Kudin, K. N.; Scuseria, G. E. *J. Am. Chem. Soc.* **2001**, *123*, 12849.
(35) Kudin, K. N.; Scuseria, G. E.; Yakobson, B. I. *Phys. Rev. B* **2001**, *64*, 235406.
(36) Jaffe, R. L. *J. Phys. Chem. B* **2003**, *107*, 10378.
(37) Wilkins, R.; Pulikkathara, M. X.; Khabashesku, V. N.; Barrera, E. V.; Vaidyanathan, R. K.; Thibeault, S. A. *Mater. Res. Soc. Symp. Proc.* **2005**, *851*, 267.

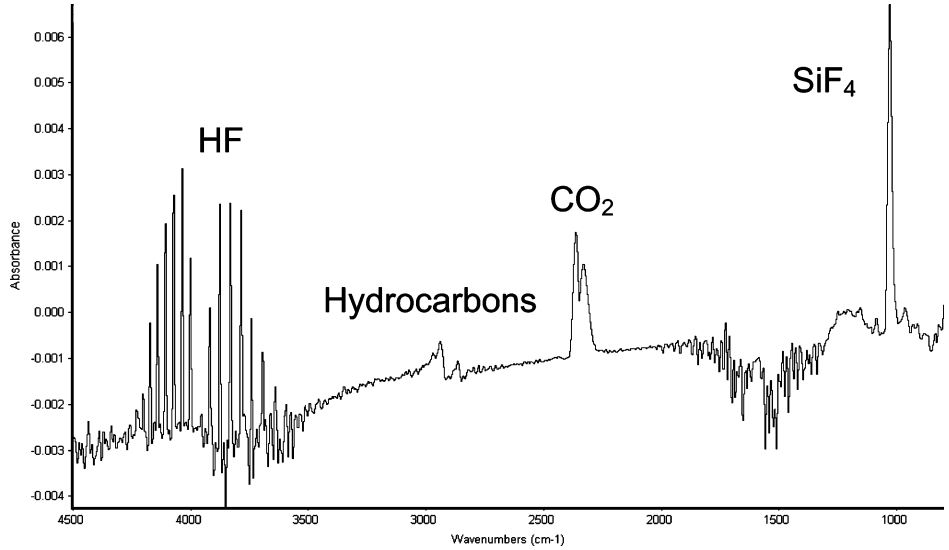

Figure 6. IR spectrum of gaseous products evolved from the 5 wt % F−SWNT/polyethylene composite during the TGA−FTIR analysis in flowing nitrogen in the 200−300 °C temperature range.

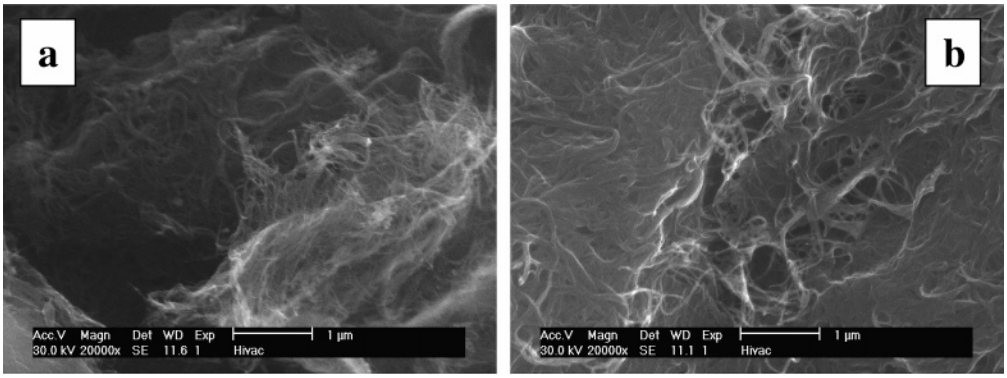

Figure 7. SEM images of the TGA residues from the composite samples of 5 wt % F−SWNT/polyethylene (a) and 5 wt % P−SWNT/polyethylene (b). The images show unchanged lengths of nanotubes consolidated into a mat of ropes.

Further supporting information about partial defluorination and the F−SWNT/polyethylene interaction taking place during melt processing by shear mixing is obtained by analyzing the evolved gases collected during TGA−FTIR experiments from the 5 wt % F−SWNT/polyethylene composite under flowing nitrogen. It was found that the residual fluorine functional groups start to detach as HF at temperature as high as 185 °C, above the polyethylene melting temperature of approximately 110 °C. The most detectable evolution of HF gas in the TGA−FTIR experiments is observed within the 200−300 °C range, as shown in the IR spectrum in Figure 6, which means that complete defluorination is less likely to occur during shear mixing melt processing of this composite. The observation of SiF_4 in this spectrum (Figure 6) is due to etching of quartz tubing material by HF. Small traces of detected hydrocarbon species indicate some initial depolymerization of PE matrix. No significant amount of fluorinated carbon species was detected in the evolved gases, suggesting that the nanotubes do not degrade. The evolution of HF seems to be independent of the nature of flowing gas (nitrogen or air) used in the TGA because in a previous work done with flowing air, the evolution of HF was observed at the same temperature.[38]

HF evolution represents a different defluorination pattern than one observed previously for the neat F−SWNTs (not surrounded by a polyethylene matrix).[4] When heated in an argon atmosphere, the neat F−SWNTs decompose in two steps. Between 300 and 560 °C CO_2 and COF_2 evolved, and above 560 °C CF_4 was observed as the main product. Fluorinated carbon gases indicated that parts of the nanotubes are destroyed, and after heating to 1000 °C, the remaining nanotubes are cut into shorter segments with an average length of 40 nm. The shorter lengths are expected to provide less mechanical reinforcement to the polymer matrixes than the original nanotubes.

However, the nanotubes are found not to be shortened during the TGA experiments done in the present work. The TGA residues from both the P−SWNT and F−SWNT/polyethylene composite samples appear as mats of long nanotube ropes as shown in Figure 7. Neither sample required gold coating for preventing charging, indicating that the intrinsic nanotube conductivity is restored even to the residue from the F−SWNT composite. Previous attempts to image F−SWNTs by SEM required gold coating or environmental mode to compensate for the low conductivity. The Raman

(38) Shofner, M. L.; Vaidyanathan, R.; Green, C.; Condon, C.; Phillips, T.; Barrera, E. V. In *Proceedings of the 9th International Conference on Composites Engineering*; Hui, D., Ed.; International Community for Composites Engineering at the University of New Orleans: San Diego, CA, 2002; Vol. 9, p 719.

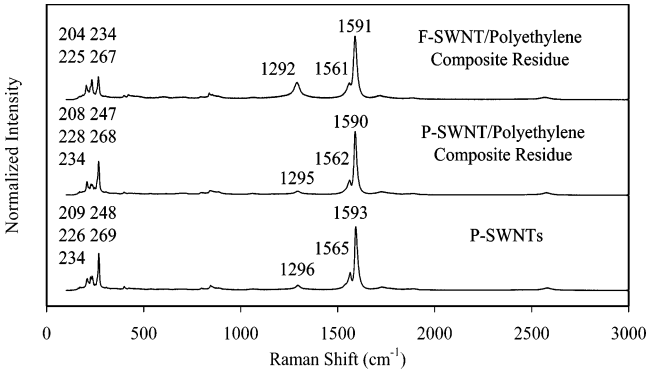

Figure 8. Raman spectra of P−SWNTs and TGA residues from the 5 wt % F−SWNT/polyethylene and 5 wt % P−SWNT/polyethylene composite samples. The features of P−SWNTs are seen in both samples. The F−SWNT composite residue shows an increase in the sp^3 carbon peak intensity as compared to that of the original P−SWNTs. The increase was attributed to minor nanotube sidewall damage during defluorination.

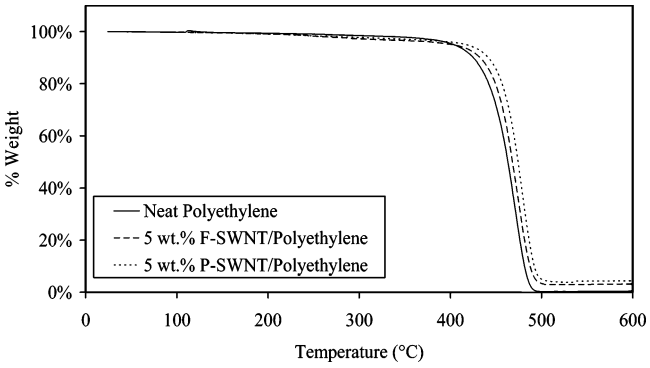

Figure 9. TGA data (in nitrogen) for neat polyethylene and composites fabricated of 5 wt % F−SWNT/polyethylene and 5 wt % P−SWNT/polyethylene. The addition of F−SWNTs and P−SWNTs does not drastically change the onset of degradation or the major degradation step. The slight increases in thermal stability of the composites are related to nanotube carbon concentration.

spectrum of the TGA residue from the P−SWNT/polyethylene composite sample is identical to that of the P−SWNTs, but in case of the F−SWNT/polyethylene TGA residue a higher intensity disorder peak at 1292 cm^{-1} is observed (Figure 8). The increase in the disorder mode is likely caused by partial damage to the nanotube sidewalls during defluorination.[9,29] The detection of a small amount of fluorinated carbon gases in the TGA−FTIR experiments supports this assumption.

The TGA experiments done in flowing nitrogen demonstrate that the P−SWNTs and F−SWNTs do not decrease the thermal stability of the polyethylene. Figure 9 shows the degradation curves for the neat polyethylene and composites fabricated of 5 wt % F−SWNT/polyethylene and 5 wt % P−SWNT/polyethylene by melt shear mixing (the TGA curve for 1.5 wt % SWNT composites is not presented on this figure). Table 1 lists the numerical details of each analysis; each value is the average of two analysis runs. The melting temperature data is taken from the temperature difference data, and the inflection point is taken as the peak of the derivative percent weight loss curve. The shape of the decomposition curves is similar for all analyzed materials, but in the particular case of the composite materials the curves are shifted to slightly higher temperatures. The 5 wt % P−SWNT/polyethylene composite produces the most notable change in degradation behavior by increasing the

Table 1. TGA Numerical Data Showing the Increase in Inflection Temperature with Increasing Nanotube Concentration in the Composites

material	melting temp (°C)	inflection temp (°C)	residual weight (%) at 600 °C
neat polyethylene	110.7	470.7	negligible
1.5 wt % F−SWNT/polyethylene	110.7	470.7	negligible
1.5 wt % P−SWNT/polyethylene	110.4	475.9	0.95
5 wt % F−SWNT/polyethylene	110.7	474.7	2.99
5 wt % P−SWNT/polyethylene	109.5	478.8	3.92

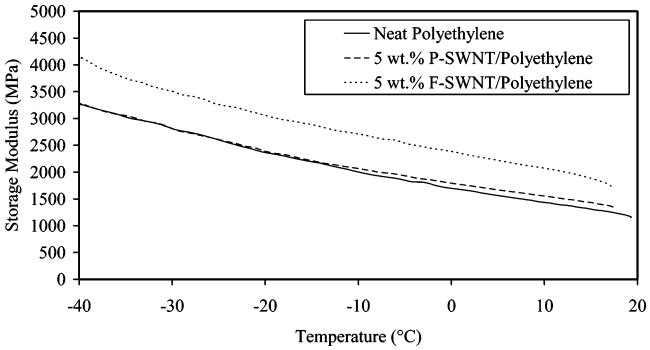

Figure 10. Measured by DMA storage modulus at 15 °C of neat polyethylene and 5 wt % F−SWNT/polyethylene and 5 wt % P−SWNT/polyethylene. The 5 wt % F−SWNT/polyethylene composite shows improved mechanical properties when compared to those of the neat polyethylene.

inflection temperature approximately by 8 deg compared to that of the neat polyethylene. The F−SWNT-containing composites show smaller differences in the thermal behavior than their P−SWNT counterparts because of a lower loading of carbon nanotube component. As mentioned previously, the F−SWNT composites contain fewer nanotubes than the P−SWNT composites at equal loadings. Because fluorine mass is included into the F−SWNT weight, a lower carbon loading would account for the difference.

The results of the DMA measurements demonstrate a larger scale property improvement of the polyethylene composites due to the addition of fluorine-functionalized SWNTs than the TGA experiments. For composite materials, observations of changes to storage modulus and tan delta are indicative of the fiber/matrix interface interactions.[39,40] A simultaneous increase in storage modulus and decrease in tan delta with respect to the neat polymer indicate the presence of a load-transferring interface because the stiffness is increased and the damping is decreased.

The observed by DMA differences in storage modulus values provide evidence of an improved interaction between the F−SWNTs and the polyethylene matrix when compared to that of the P−SWNTs/polyethylene composite. As shown in Figure 10, all composite materials except the 5 wt % F−SWNT/polyethylene composite show a similar storage modulus at 15 °C. The 5 wt % F−SWNT/polyethylene composite shows distinct improvement over the neat polyethylene with an average increase of 44%. The changes in the storage modulus of the other three composite materials cannot be separated from the error bars. The enhancement is constant to −40 °C as shown in Figure 11.

(39) Liang, J. Z.; Li, R. K. Y.; Tjong, S. C. *Polym. Int.* **1999**, *48*, 1068.
(40) Liang, J. Z.; Tang, C. Y.; Li, R. K. Y.; Tjong, S. C.; Yung, K. C. *Key Eng. Mater.* **1998**, *145−148*, 817.

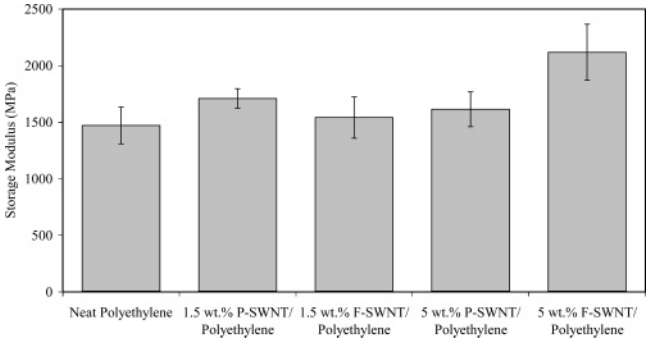

Figure 11. Measured by DMA storage modulus of the neat polyethylene and 5 wt % F−SWNT/polyethylene and 5 wt % P−SWNT/polyethylene. The addition of F−SWNTs increases storage modulus, whereas the addition of P−SWNT provides no mechanical reinforcement.

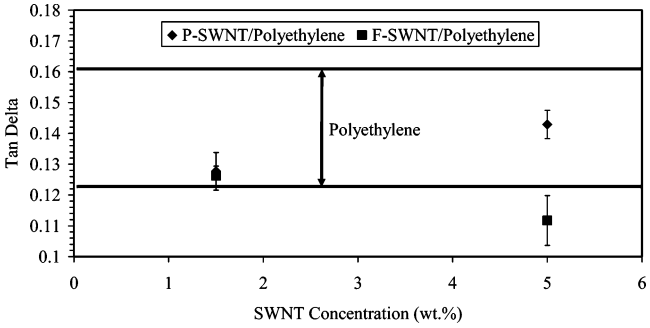

Figure 12. Tan delta values at 15 °C measured by DMA for neat polyethylene and polyethylene composites. The bold lines indicate the upper and lower limit values for the polymer. The F−SWNT composites show decreased damping with increasing concentration, but the P−SWNT composites show a saturation behavior.

The behavior of tan delta supports the conclusion that the interfacial load transfer is greater in the F−SWNT composite. The damping ability of the polymer is decreased with increasing F−SWNT concentration as shown in Figure 12. The load of 1.5 wt % P−SWNT also decreases tan delta, but as the concentration increases to 5 wt %, the tan delta value is approximately the same as for the neat polyethylene. The similar trend can also seen in the storage modulus data shown in Figure 11. This is likely due to a decreased dispersion in the polymer matrix as the P−SWNT concentration increases.[24,41]

Conclusion

The studies of the nanotube−polyethylene composites clearly indicate that fluorination provides a means to disrupt the larger SWNTs rope structure and create an opportunity for direct covalent bonding between the nanotubes and the polyethylene matrix. Both effects improve the interfacial characteristics and mechanical properties of the fluorinated nanotube composites with respect to the corresponding purified nanotube composites as evidenced by the dynamic mechanical properties. This result shows the versatility of covalent functionalization in general to act as an efficient aid in dispersing and to provide a removable functional groups for in situ cross-linking. These initial results present a universal mechanism for using covalent functionalization to create fully integrated SWNT composites in situ and construct novel chemical architectures to achieve further increases in multifunctional properties.

Acknowledgment. This research was funded by the NSF Graduate Fellowship Program, Welch Foundation Grant C-1494, and NASA Grants NGT9-23, NCC9-77, and NCC-1-02038. This work made use of the TCSUH/MRSEC Shared Facilities supported by the State of Texas through the Texas Center for Superconductivity at the University of Houston and by the National Science Foundation under Award Number DMR-9632667. The authors also thank Dr. Z. Gu for help with the TGA−IR experiments, Dr. H. Peng and Professor J. L. Margrave for fluorinating the nanotubes, and Dr. S. Ramesh for helpful discussions.

CM051475Y

(41) Valentini, L.; Biagiotti, J.; Kenny, J. M.; Lopez Manchado, M. A. *J. Appl. Polym. Sci.* **2003**, *89*, 2657.